



122
653
THS

ELASTIC-PLASTIC TRANSITION TESTS
ON VARIOUS ROCK TYPES

Thesis for the Degree of M. S.
MICHIGAN STATE UNIVERSITY
Athipet Bashyam Raman
1962

This is to certify that the

thesis entitled

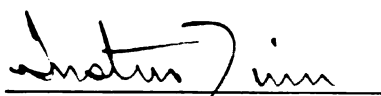
ELASTIC-PLASTIC TRANSITION
TESTS ON VARIOUS ROCK
TYPES

presented by

Athipet Bashyam Raman

has been accepted towards fulfillment
of the requirements for

M.S. degree in Geology


Major professor

Date Dec 31 1962

O-169



ABSTRACT

ELASTIC-PLASTIC TRANSITION TESTS ON VARIOUS ROCK TYPES

By Athipet Bashyam Raman

Rocks in general behave as a brittle material when subject to low confining pressure. But as the confining pressure is increased, they are found to exhibit plastic behavior.

In the conventional methods, the confining pressure is applied by subjecting the rocks to a liquid confining medium. A new technique invented by Serata develops the confining pressure in a cylindrical sample of rock by enclosing the same in a tightly fitted steel cylinder and compressing the specimen axially. Thus triaxial pressure is developed in the specimen as there is strain restriction in all directions. By employing this method, called the transition test, Serata obtained plastic state of deformation in paraffin and rock salt, and the change from elastic to plastic state was found to be abrupt. From the relationship between the lateral stress and axial stress, he was able to obtain the octahedral shearing strength of the materials tested.

Morrison improved this technique in his studies on rock salt by applying better friction reducers and also obtained values for elastic constants.

In this work the earlier triaxial tests on rock types are summarized and the new technique of transition test is reviewed along with the method of obtaining the octahedral shear strength and elastic constants.

Successive cycles of loading were conducted on limestone, sandstone, granite, marble, shale, anhydrite, and rock salt reaching high pressures up to a maximum of 110,000 psi and the relationships between lateral and axial stresses were studied.

Evaluation of the test results show that there is a general trend in transition from elastic to plastic state, though it may not be very abrupt. All rocks except salt show a gradual transition. The slopes of the plastic lines are much smaller than the theoretical prediction. This difference may be attributed to the nature of the strength of grains and of their mutual bonding.

ELASTIC-PLASTIC TRANSITION TESTS ON
VARIOUS ROCK TYPES

By

Athipet Bashyam Raman

A THESIS

Submitted to
Michigan State University
in partial fulfillment of the requirements
for the degree of

MASTER OF SCIENCE

Department of Geology

1962

32136
2/2/11

ACKNOWLEDGEMENTS

The author desires to express his sincere thanks to his major professor Dr. Justin Zinn, Professor, Department of Geology, for his valuable suggestions and careful scrutiny of the manuscript. Special thanks are also due to the National Science Foundation under whose research project the present work was carried out. The author is particularly indebted to the director of the project, Dr. Shosei Serata, Assistant Professor of Civil Engineering, for his constant and clear sighted guidance. Grateful thanks are also due to Mr. Shunsuke Sakurai, Graduate Assistant, Civil Engineering Department, for his assistance in conducting the experiments and analyzing the results. Gratitude is also extended to Dr. Leonard Obert, U. S. Bureau of Mines, College Park, Maryland, and to the Michigan State Geological Survey, for supplying the core samples from which the specimens were machined for the tests.

CONTENTS

	Page
Acknowledgements	ii
List of Figures	iv
List of Symbols	vi
Chapter	
I. Introduction	1
II. Summary of Triaxial Tests on Rocks	3
III. Theory of the Experiments	8
IV. Testing Method	19
V. Specimen Description and Testing Results	30
VI. Evaluation of Experimental Results and Discussion.	44
VII. Conclusions	48
VIII. Suggestions for Additional Research	50
Bibliography	51

LIST OF FIGURES

Figure		Page
1.	Mohr's diagram representing underground stress conditions	9
2.	Relation of axial and lateral stresses in transition test	15
3.	Cutaway view of the thick-walled cylinder with the enclosed specimen	20
4.	Photograph of the testing machine in operation	22
5.	Photograph of the testing cell with the strain gages attached and of the specimen with the plungers.....	23
6.	Illustration of the strain gage locations on the thick-walled cylinder	24
7.	Strain gage wire diagram	25
8.	Photograph of the specimens tested	31
9.	Lateral stress - axial stress diagram showing loading cycles I, III, and V on limestone	32
10.	Lateral stress - axial stress diagram showing loading cycles I, III, and V on sandstone	33
11.	Lateral stress - axial stress diagram showing loading cycles I and III on granite	35
12.	Lateral stress - axial stress diagram showing loading cycles I, II, and III on marble	36
13.	Poisson's ratio versus loading; cycles I to III; marble	37
14.	Modulus of elasticity versus loading; cycles I to III; marble	38

Figure		Page
15.	Lateral stress - axial stress diagram showing loading cycles I and II on shale	39
16.	Lateral stress - axial stress diagram showing loading cycles II and III on anhydrite	40
17.	Lateral stress - axial stress diagram showing loading cycles I and II on rock salt 'A'	42
18.	Lateral stress - axial stress diagram showing loading cycles I and II on rock salt 'B'	43

LIST OF SYMBOLS

A	ratio of lateral stress to axial stress in the elastic state
α	angle of elastic line
β	angle of plastic line
c	internal radius of thick-walled cylinder
d	external radius of thick-walled cylinder
E	modulus of elasticity
E_R	modulus of elasticity of rock
E_s	modulus of elasticity of steel
e_1	strain in axial direction
e_2	strain in lateral direction
e_3	strain in lateral direction
e_t	tangential strain in the external surface of the thick-walled cylinder
e_z	axial strain in specimen
Γ	ratio of axial strain to lateral strain in the elastic state
K_o	maximum octahedral shearing strength
P_i	uniform internal pressure on the cylinder
P_o	uniform external pressure on the cylinder
ϕ	coefficient of internal friction of the material
S_L	lateral stress in specimen

S_z	axial stress in specimen
σ_1	major principal stress
σ_2	intermediate principal stress
σ_3	minor principal stress
σ_m	mean principal stress
σ_n	normal stress perpendicular to failure plane
σ_t	tangential stress developed in the external surface of the thick-walled cylinder
σ_θ	tangential stress at radius r
τ	shear stress acting in the plane of failure
τ_c	true shearing strength which is constant for a given material
τ_o	octahedral shear stress
v	Poisson's ratio
v_R	Poisson's ratio of rock
v_s	Poisson's ratio of steel
w	apparent coefficient of internal friction of a material under conditions of restraint in lateral expansion

INTRODUCTION

Most rocks are exceedingly brittle when deformed under ordinary atmospheric pressure conditions. But these very same rocks exhibit a large amount of flow deformation as revealed in the highly contorted sections of the earth's crust. This increase in ductility is considered to be due to the environmental conditions existing deep in the crust, the conditions being high confining pressure, high temperature, stress differences and the presence of hydrothermal solutions. That confining pressure plays an important role in bringing about the transition from brittle to ductile flow was first proved by Adams and Nicolson [1] (1901), Adams [2, 3] (1910, 1912), and Adams and Bancroft [4] (1917). Later, Griggs [8] (1936), Balsley [5] (1941), Bridgeman [6] (1949a), Robertson [16] (1955), Handin and Hager [11] (1957), and Paterson [15] (1958a) have all illustrated the same quantitatively with improved techniques.

To subject the rocks under high pressure conditions, the above investigators used a liquid confining medium and the specimen was put to differential stress by means of pistons acting axially on the ends of specimens. Instead of confining the specimen to a liquid confining medium, Serata [7] (1961) has devised a very simple triaxial technique in which the cylindrically cut specimen is exactly fitted in a cylindrical steel cell. The specimen is then subjected to axial pressure by means of pistons. Under this set up, a triaxial pressure condition is attained

as the lateral expansion of the specimen under axial stress is restrained by the confining steel cell. By applying this technique, Serata obtained plastic deformation in paraffin and rock salt and also showed that under such conditions of restraint of lateral strain, the transition from elastic to plastic state in the rock is abrupt. This testing method is called by him the "Transition Test." From this method he also derived values for octahedral shearing strength for the materials tested. This octahedral shearing strength measures the intensity of stress which is needed to bring a solid substance into a plastic state.

By applying this technique on rock salt and with additional relations and instrumentation, Morrison [14] (1962) obtained values of Poisson's ratio, modulus of elasticity, and compressibility for the materials tested.

The object of the present study is to test a number of rock samples of varying strength under this new technique, to evaluate the relationship between the lateral and axial stresses in the specimens and to compare the trend in transition from elastic to plastic state in the different rock types. The specimens tested are limestone, sandstone, granite, marble, shale, anhydrite and rock salt.

II. SUMMARY OF TRIAXIAL TESTS ON ROCKS

Since the beginning of this century, extensive experiments have been carried out on the deformation of rocks. It has been known for some time that the rocks become stronger and more ductile with the application of confining pressure.

The earliest pioneers in the field were Adams and his collaborators [1] (1901), [2] (1910), [3] (1912), [4] (1917) who had established at least qualitatively that both the ultimate strength and the ductility of some rocks increase with the confining pressure. This was established in experiments using constraining steel tubes.

Von Karman [20] (1911) was the first to perform the triaxial tests under a truly hydrostatic confining pressure. He tested Carrara marble and red sandstone in a device which permitted compressive loading of samples subjected externally to liquid pressures of several thousand atmospheres. He attained data for quantitative stress-strain curves and found that at high pressures the curves were similar to those of ductile metals which show poorly defined yield points, work hardening and large permanent deformations.

Notable contributions to rock deformation were made by Griggs [8] in 1936. He subjected solid cylinders of rocks, half inch in diameter, to triaxial compression under a liquid confining medium. The liquid

used mostly was kerosene. The specimens tested were Solenhofen limestone, marble, and quartz. In his experiments he reached pressures up to 13,000 atmospheres. The stress-strain curves obtained by him for limestone and marble show the well established effects of pressure on strength and ductility. The earlier specimens that he tested wereunjacketed, but when jacketed they showed only a 40 per cent increase in strength. Even at the highest confining pressures that Griggs was able to attain, he was not able to produce continuous flow in any of the materials tested. However, he states, "as the confining pressure is increased the physical character changes gradually from dominantly brittle to dominantly plastic. No sharp line can be drawn between the two." Further, he found that (1) for each material, the value of the elastic limit obtained with the highest confining pressures was only 10 percent greater than that observed at the lowest pressures; and that (2) the ultimate compressive strength of marble increased about 1,400 per cent in the same series of tests.

Balsley [5] (1941) made extension tests on marble under pressures up to 1000 atmospheres. The stress-strain relations were suggestive of ductile behavior.

Griggs and his collaborators [9] (1951), [12] (1951), [19] (1951) at the University of California have made a detailed study on the deformation of Yule marble. Their earlier studies were conducted at room

temperature under a 10,000 atmosphere confining pressure. Their analysis of data, together with the observed micro-fabric changes, proved to be an aid in establishing the deformation mechanism involved, twinning planes, gliding planes etc. Their later investigations (Griggs, Turner, and Heard [10] 1960) in triaxial tests were performed under high temperatures ranging from 500°C to 800°C . Varieties of rocks like pyroxenite, peridotite, basalt, granite, dolomite, marble, quartz crystals and other aggregates were tested. They have reported the strength of these as a function of temperature.

Bridgman [7] (1952) has made some extensions tests on rocks under extreme pressures up to 30,000 atmospheres. He obtained a 20 per cent reduction of area in his extension experiment on a rock salt at a load of 510 kg/cm^2 . For Solonhofen limestone he measured a 53 per cent reduction of area at a load of $14,000 \text{ kg/cm}^2$.

Robertson [16] (1955) has made deformation tests on limestone, sandstone, marble, slate, quartzite, granite, diabase and other rocks. He also tested minerals like pyrite, quartz, microcline and fluorite. He reached pressures up to 4,000 atmospheres. His tests included compression of solid cylinders, crushing of hollow cylinders, and punching of disks. He found all rocks exhibited a range of elastic linearity of stress with strain. He showed that limestones and marbles could be made to flow plastically to large deformations. His heating experiments

on limestones demonstrated an increase in plasticity with a rise in temperature. But he found no plastic behavior for the silicate rocks and minerals tested.

Handin and Hager [11] (1957) in connection with their work with the Shell Development Company have performed a number of triaxial tests on dry sedimentary rocks at room temperature and at various confining pressures ranging from 0 to 2,000 atmospheres. The rock types tested were siltstone, shale, sandstone, limestone, dolomite, and anhydrite. Their tests reveal small increases in elasticity and yield stress and large increases in ultimate strength under pressure. Most rocks also show some increase in ductility.

Serata [17] (1961) and his collaborators in the Engineering Research Division of Michigan State University have studied the triaxial behavior of paraffin, rock salt, and dolomite under the new triaxial technique of confining the specimen in a closely fitted steel cell and then applying axial pressure. The new technique is definitely more advantageous than the conventional triaxial tests conducted under liquid medium. This new method is very simple, inexpensive, accurate, and allows a very high pressure capacity. By applying this technique and from the study of the materials tested, Serata has postulated a new theory regarding the transition from elastic to plastic state in rocks. He arrives at the following conclusions on the static stress conditions:

1. The static stress field in underground formations can be calculated if the octahedral shearing strength and the Poisson's ratio of the formations are known.
2. In underground formation, the state of stress should be either elastic or plastic, and no intermediate state should exist. Therefore, the plastic state is distinguished from the elastic state by a definite boundary of transition between the two states.
3. In a homogeneous formation, there should be a plane of the transition boundary from elastic to plastic with increasing depth.
4. No hydrostatic state of stress exists in an underground formation, although the state of stress approaches the hydrostatic condition with increasing depth beyond the transition boundary.
5. The transition of the states between plastic and elastic is caused by an abrupt change in the mechanism of yielding in underground formations.

Recently in Salzburg, Austria, John [13] (1962) has developed a new approach to the study of triaxial compression of rocks. This new technique involves the compression of rocks of standard dimensions in situ. The detailed results of his experiments are awaited. He postulates that the analysis of his test results will help in practical design problems and in the estimation of overbreaks in rock excavations for tunnelling.

III. THEORY OF THE EXPERIMENTS

It is a well known fact that rocks generally exhibit varying degrees of plastic nature under progressive increase of triaxial compression. This phenomenon is explained by solid state mechanics as molecular (or ionic) displacement taking place in solids when the shearing stress exceeds a definite limit of the intermolecular attraction. From studies of triaxial behavior of materials under conditions of controlled triaxial strain, a new theory of transition from elastic to plastic state has been proposed by Serata. The development of this theory is briefly outlined below.

Rocks, though they exhibit a brittle behavior under uniaxial loading, become increasingly plastic under triaxial loading. This change of character can be visualized by means of a Mohr diagram.

The Mohr diagram of a material represents the locus of stress conditions which bring about the failure of the material. The results of triaxial compression on a material can be shown in a Mohr diagram as shown in figure 1. The principal stresses are plotted in the abscissa and the shearing stresses on the ordinates. The semicircles indicate the yielding conditions of the material, and the envelope obtained is the result of a number of triaxial yielding tests in a large range of mean principal stress. The mean principal stress is the average of the three principal stresses:

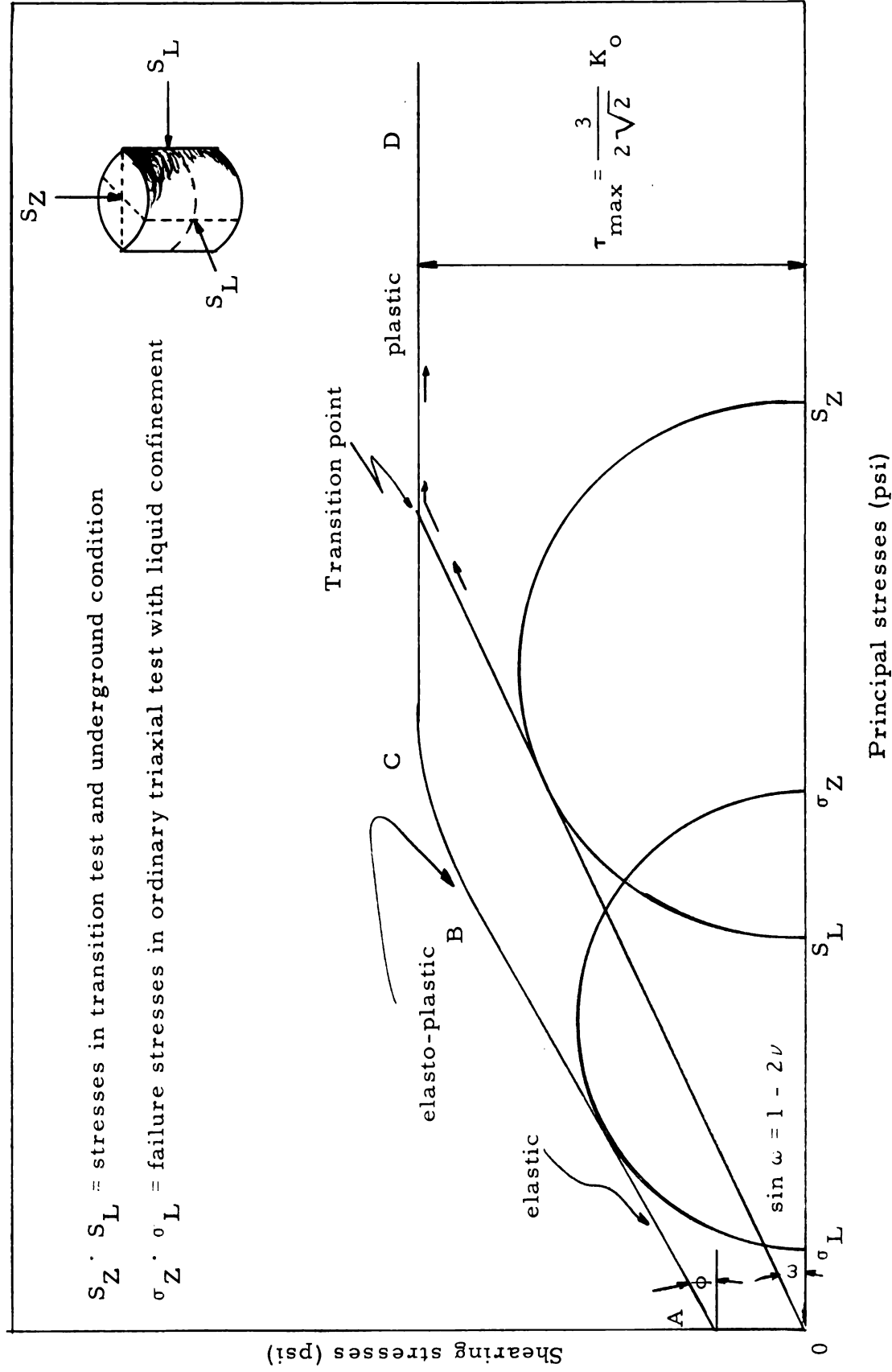


Figure 1. Mohr's diagram representing underground stress conditions

$$\sigma_m = \sigma_1 + \sigma_2 + \sigma_3 \text{ where } \sigma_1, \sigma_2, \text{ and } \sigma_3 \text{ are principal stresses} \quad (1)$$

A study of the Mohr envelope reveals that it consists of three parts. The first part AB has a definite slope, i. e. , it has a definite value of $\tan \theta$ within a certain limit on the mean principal stress. This part illustrates the Coulomb-Mohr theory of triaxial failure and applies to brittle state only. Here the coefficient of internal friction remains independent of normal stress. The state of stress can be represented as:

$$\tau_c \geq \tau - \phi \cdot \sigma_n \quad (2)$$

where

τ_c = true shearing strength which is a constant for a given material;

τ = shear stress acting in the plane of failure;

ϕ = coefficient of internal friction of the material;

σ_n = normal stress perpendicular to the failure plane.

In the above equation $>$ sign indicates a stable state and the $=$ sign represents a failure or yielding state.

The second portion BC of the envelope shows a gradual decrease in the slope, finally leading into the third part where the envelope reaches horizontality. The second portion represents an intermediate stage called the elasto-plastic or plasto-elastic state.

In the third portion, CD in the figure, the envelope, as aforesaid is horizontal. This portion represents the condition of plasticity defined by Henky and von Mises, based on the energy of distortion theory. According to this theory, every material has a maximum limit in strain energy of distortion beyond which it becomes plastic. The strain energy is obtained by subtracting the elastic energy of volume expansion from the total elastic energy stored in a material. This leads to the octahedral shearing stress theory of failure which makes it possible to apply the energy of distortion theory of failure by dealing only with stresses instead of dealing with energy directly. This theory states that a material becomes plastic when the shear stress on an octahedral shearing surface reaches a maximum limit K_o which is called the octahedral shearing strength of the material and which is specific to the material concerned. The octahedral shear stress τ_o can be expressed as a function of the three principal stresses:

$$\tau_o = \frac{1}{3} \sqrt{(\sigma_1 - \sigma_2)^2 + (\sigma_2 - \sigma_3)^2 + (\sigma_3 - \sigma_1)^2} \quad (3)$$

For example, taking a simple case, as when the minor principal stresses are made equal such that $\sigma_1 > \sigma_2 = \sigma_3$, the equation 3 becomes

$$\tau_o = \frac{\sqrt{2}}{3} (\sigma_1 - \sigma_3) \quad (4)$$

If the stress remains at the constant K_o , in a plastic state, the maximum shearing stress $\tau_{\max} = \frac{\sigma_1 - \sigma_3}{2} = \frac{3}{2\sqrt{2}} K_o$ (5)

The projection of this equation 5 in the Mohr diagram plots a horizontal line representing the horizontal portion of the Mohr envelope.

Considering the state of stress in a confined medium as in underground formations, the following relationships between the principal stresses and the principal strains may be applied.

$$\begin{aligned} e_1 &= \frac{1}{E} [\sigma_1 - \nu (\sigma_2 + \sigma_3)] \\ e_2 &= \frac{1}{E} [\sigma_2 - \nu (\sigma_1 + \sigma_3)] \\ e_3 &= \frac{1}{E} [\sigma_3 - \nu (\sigma_1 + \sigma_2)] \end{aligned} \tag{6}$$

where

e_1 = strain in axial direction

e_2 = strain in lateral direction

e_3 = strain in lateral direction

σ_1 = stress in axial direction

σ_2, σ_3 = stress in lateral direction

E = modulus of elasticity

ν = Poisson's ratio

Assuming that there is no tectonic pressure, the lateral stress is created only by the restriction of lateral expansion of the compressed mass by the vertical stress. No lateral deformation is possible as the lateral extent of the medium is almost infinite. If such lateral strain restrictions are assumed, the stress-strain relationships will be:

$$\begin{aligned}
\sigma_1 &= S_Z = \text{vertical stress} = \text{overburden pressure} \\
\sigma_2 &= \sigma_3 = S_L = \text{lateral stress} \\
e_1 &= e_Z = \text{vertical strain} \\
e_2 &= e_3 = 0 = \text{lateral strain}
\end{aligned} \tag{7}$$

Substitution of these values into equation 6 will result in the following expression in terms of overburden pressure:

$$S_L = \frac{\nu}{1 - \nu} \cdot S_Z \tag{8}$$

This equation 8 shows that the lateral stress S_L and the vertical stress S_Z are related only by a single quantity, viz., the Poisson's ratio for elastic conditions. This relation is expressed in a Mohr diagram as a straight line with a definite slope w (figure 1). This straight line is a tangent drawn from the origin to a Mohr circle whose major and minor principal stresses being S_Z and S_L respectively and the angle of slope w is

$$\sin w = \frac{(1 - \frac{\nu}{1-\nu})}{(1 + \frac{\nu}{1-\nu})} = 1 - 2\nu \tag{9}$$

It is seen from figure 1 that the straight line cuts the horizontal (plastic yielding) portion of the envelope. This relationship is true for all rock types since the angle w of rocks ranges between 15° and 45° while the angle ϕ of the coefficient of internal friction ranges between 50 to 80° [21] (1959). It is from this relation of the straight line of the

elastic state cutting the horizontal line (plastic state) of the Mohr envelope and from the fact that there is no stable condition beyond the envelope that Serata postulated the transition from the elastic state to the plastic state as an abrupt one. This abrupt transition should be exhibited by all types of underground formations.

Based upon the above postulation, a direct relation between the vertical and lateral stresses in underground formations can be attempted as shown in figure 2. The vertical stresses S_Z and the lateral stresses S_L are plotted in the ordinate and abscissa respectively in terms of the octahedral shearing strength of the material K_o as a unit. In such a diagram, the elastic state of stress is represented by a straight line passing through the origin with an angle of slope α which is derived from equation 8 as

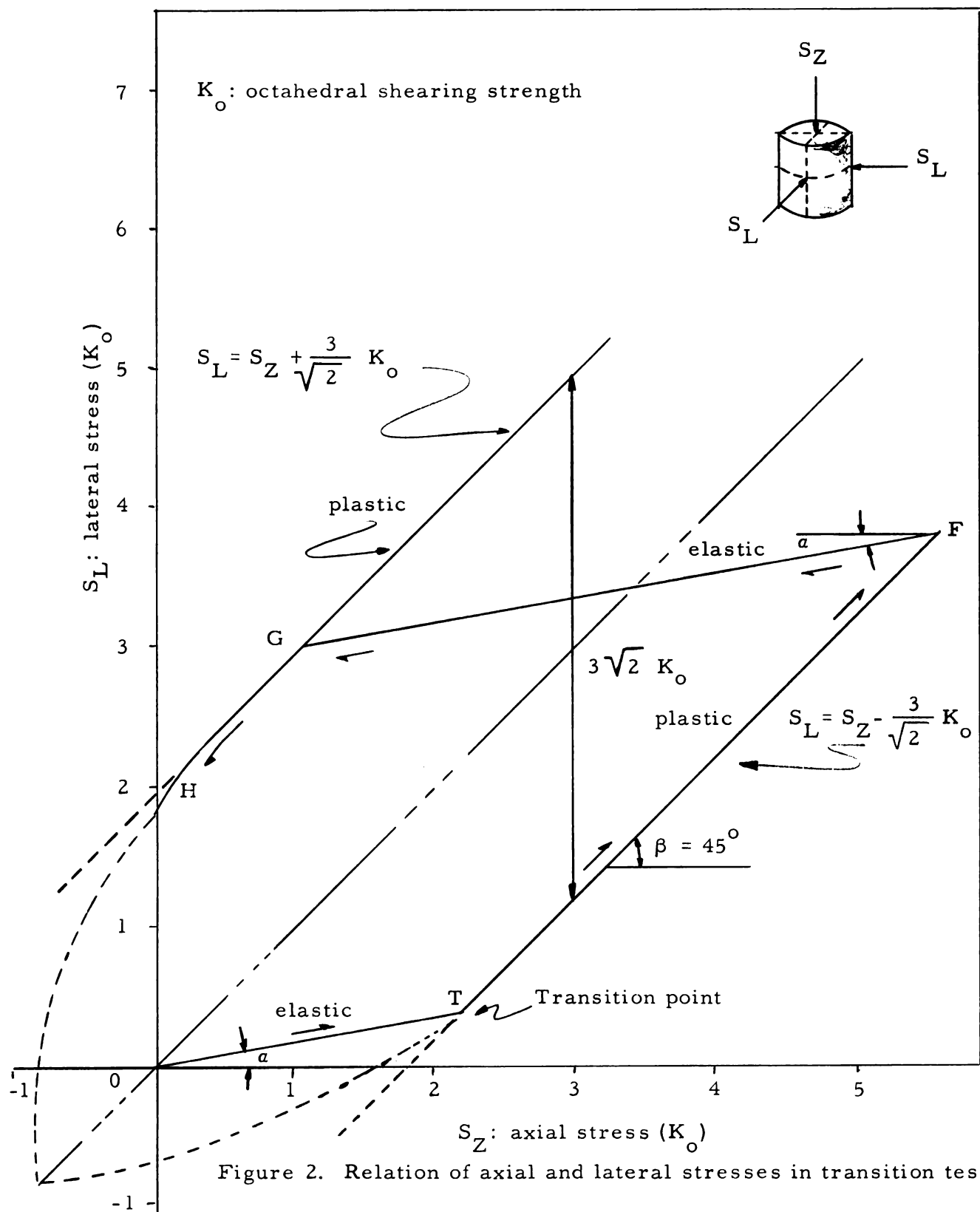
$$\tan \alpha = \frac{dS_L}{dS_Z} = \frac{v}{1-v} \quad (10)$$

The plastic state of stress forms another straight line with the angle of tangent $\beta = 45^\circ$. This line is derived from the equation of plastic state (equation 3) and by treating $\tau_o = K_o$ and $\sigma_2 = \sigma_3$ as:

$$S_L = S_Z + \frac{3}{\sqrt{2}} K_o \quad (11)$$

Hence

$$\frac{dS_L}{dS_Z} = \tan \beta = 1 \quad (12)$$



The above two lines determine the state of stress in underground formations with respect to increasing depth. It can be interpreted that the stress conditions of the ground remain elastic until the overburden pressure, S_Z is about $3 K_o$; but on exceeding the same the stress conditions become plastic whatever the depth. It is also seen from the figure that the S_Z/S_L relation is constant until the transformation point is reached and then on exceeding this point the ratio tends to approach 1. But it never reaches 1 as there is no hydrostatic state of stress existing in the underground formations.

From the figure it is apparent that the transition point T is easily obtained by merely plotting the vertical (axial) stress against the lateral stress. The $S_Z - S_L$ relation follows the elastic line and then swings to the plastic line after the transition point. Unlike the underground conditions, it is possible to reduce S_Z in the laboratory. On gradual reduction of S_Z it is found that the $S_Z - S_L$ relation follows the elastic line FG and then the plastic line GH. Their slopes are the same as the initial elastic and plastic lines. When the axial stress S_Z is finally reduced to zero, it is found that some lateral stress still remains in the specimen. This is illustrated by the plastic line of stress cutting the ordinate at H. The dashed curve in the figure indicates the condition of brittle failure when one of the principal stresses is zero or tensile. Further, it may be observed from the figure that the octahedral shear

strength of a material is one-third of the perpendicular distance between the lines of plastic stress.

In the above discussion it is assumed that there is no lateral strain occurring in the specimen. However, it is obvious that some lateral expansion must occur in the specimen so as to exert some strain in the confining steel cell from which all measurements of strain are recorded. However, this small lateral strain occurring in the specimen does not necessarily invalidate the theory. If the elastic constants of the specimen are to be determined, it is required to know accurately the effects of lateral expansion. The transition test data will be useful in this connection and the determination of elastic constants from the transition test is developed below [14] (1962).

Considering the effects of lateral strain, the stress conditions of equation 6 will be:

$$\sigma_1 = S_Z$$

$$\sigma_2 = \sigma_3 = S_L$$

$$e_1 = e_Z$$

$$e_2 = e_3 = e_L$$

Now, the equation 6 can be written as:

$$e_Z = \frac{1}{E_R} [S_Z - 2\nu_R S_L]$$

$$e_L = \frac{1}{E_R} [S_L - \nu_R (S_L + S_Z)] \quad (14)$$

Equations 14 can be resolved for Poisson's ratio and the modulus of elasticity as follows:

$$\nu_R = \frac{1 - \Gamma A}{2A - \Gamma (A+1)} \quad (15)$$

where

$$A = \tan \alpha = \frac{S_L}{S_Z}$$

$$\Gamma = \tan \gamma = \frac{e_Z}{e_L}$$

$$E_R = \frac{\frac{S_Z}{2S_L} - \frac{S_L}{(S_L + S_Z)}}{\frac{e_Z}{2S_L} - \frac{e_L}{(S_L + S_Z)}} \quad (16)$$

IV. TESTING METHOD

It was pointed out in the previous chapter that the abrupt change of the slope dS_L/dS_Z represents the transition point between the elastic and plastic state of a material. Hence to find this point the plotting of S_L versus S_Z must be done. These two quantities are determined by the following instrumentation.

Figure 3 shows the cutaway view of the specimen enclosed in a thick walled cylinder. The cylindrical specimen is confined exactly by the thick walled cylinder and this prevents lateral expansion. The specimen is compressed axially by means of steel plungers having the same diameter as the specimen. This condition develops axial load on the specimen only and not on the thick walled cylinder. But the application of axial load on the specimen develops lateral stress in the specimen which is simultaneously propagated into the surrounding thick walled cylinder. The lateral tangential strains thus developed in the cylinder are measured by SR-4 strain gages. The axial strains in the specimen are measured by an Ames dial gage which is mounted between the platens of the testing machine.

The apparatus used for compressing the plungers on the specimen is Tinius-Olsen testing machine. It has a capacity of 60,000 pounds in the lower range and the total applied load can be measured to the nearest

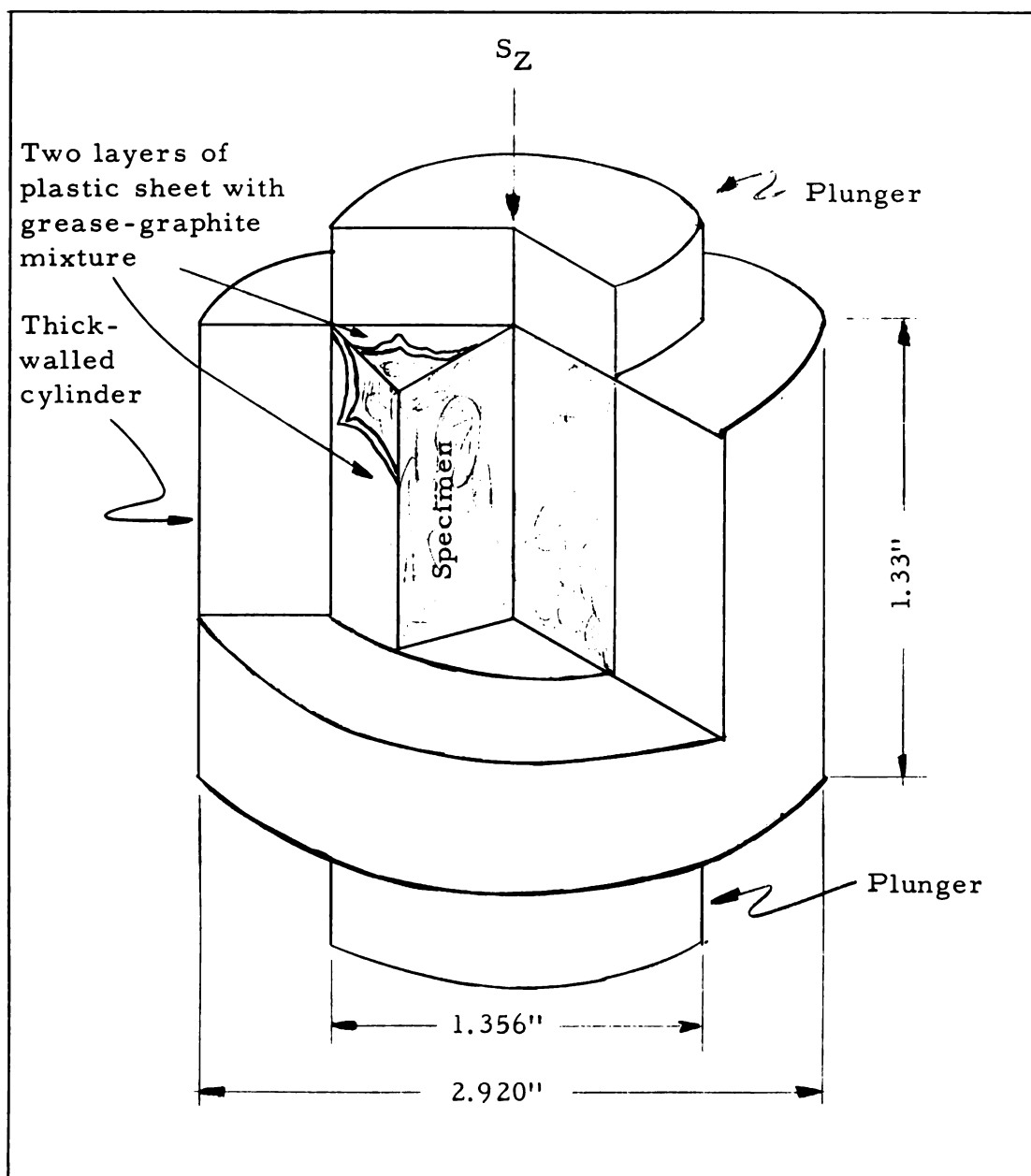


Figure 3. Cutaway view of the thick-walled cylinder with the enclosed specimen.

100 pounds. In the high range it has a capacity of 300,000 pounds and each division can be read up to the nearest 500 pounds, which amounts to 346 psi of axial pressure on the specimen. The testing machine in operation is shown in figure 4.

The thick walled cylinder used is made of high carbon steel possessing a yield strength of 235,000 psi with a modulus of elasticity of about 30×10^6 psi. The external and internal diameters of the steel cell are 2.920 and 1.356 inches respectively. The height of the cell is 1.330 inches. This steel cell is shown in figure 5 with the strain gages attached. A small cell is also used to test rocks such as shale of lesser length.

The plungers used for axial compression are made of "Keto" tool steel with a yield strength of about 325,000 psi.

The lateral and axial strains developed on the surface of the steel cell are measured by AR-1 rosette SR-4 strain gages. Three such gages are attached around the cell 120° apart in the single row along the central portion of the cell such that they are oriented with one of the three gage axes parallel to the axis of the cell and the other normal to the same. This arrangement is shown in figure 6. The wiring diagram of the strain gages is shown in figure 7.

The tangential and axial stresses developed at each gage location as a result of specimen compression can be determined from the



Figure 4. Photograph of the testing machine in operation.



Figure 5. Photograph of the testing cell with the strain gages attached and of the specimen with the plungers.

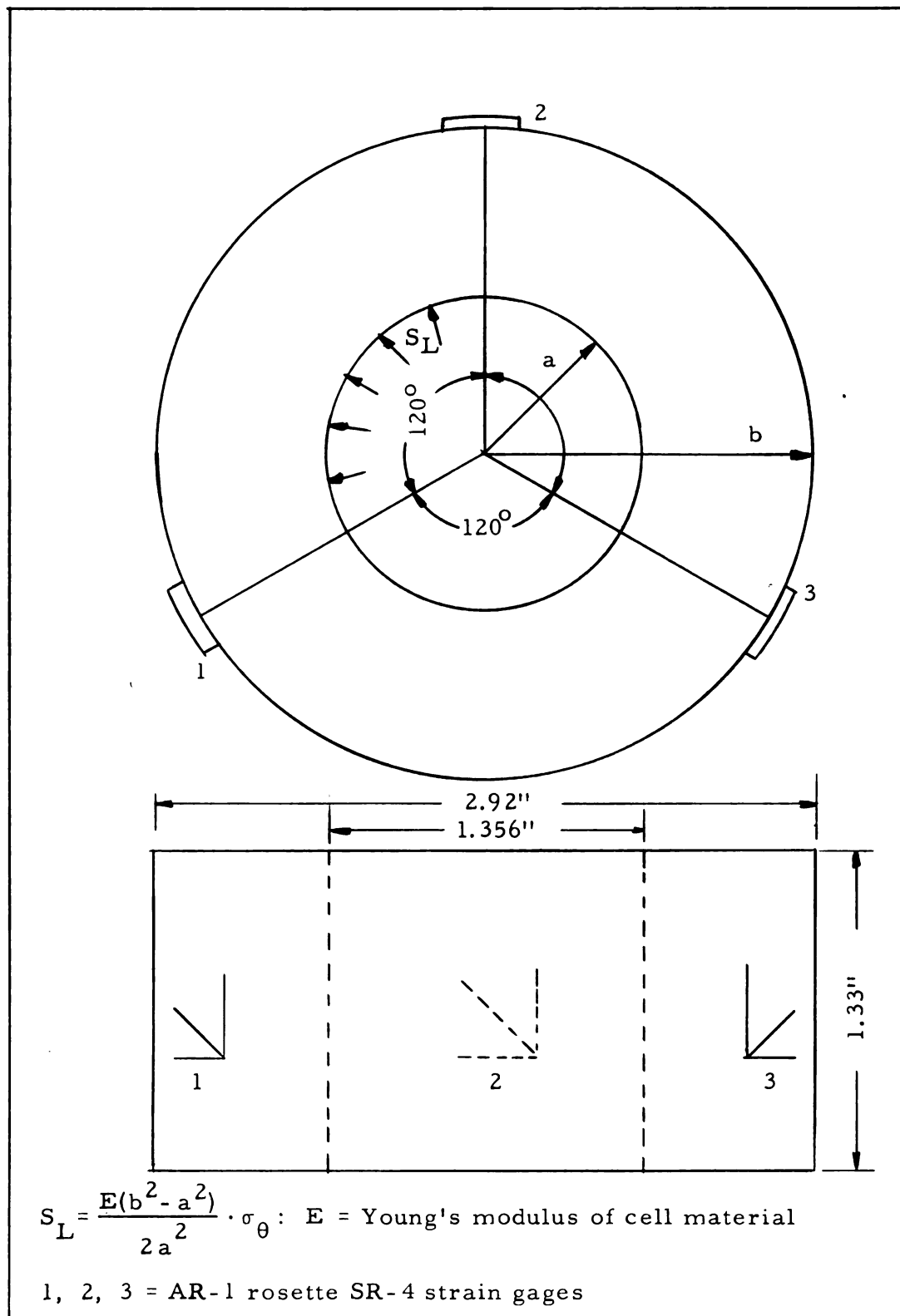


Figure 6. Illustration of strain gage location on the thick-walled cylinder

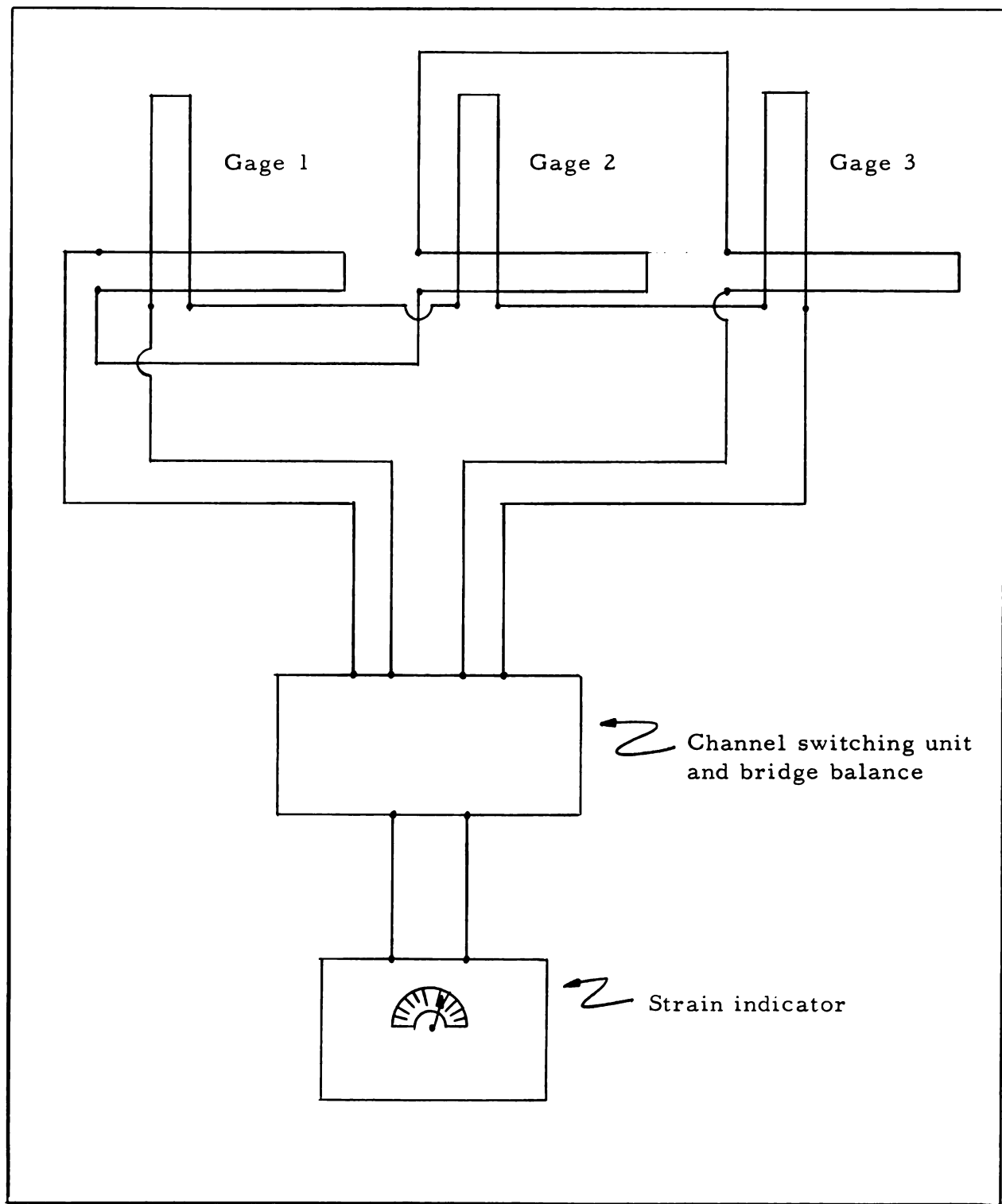


Figure 7. Strain gage wire diagram

following equations:

$$\sigma_t = \frac{E_s}{(1 - \nu_s^2)} (e_\theta + \nu_s e_Z) \quad (17a)$$

$$\sigma_Z = \frac{E_s}{(1 - \nu_s^2)} (e_Z + \nu_s e_\theta) \quad (17b)$$

The tangential stress developed in a hollow cylinder subject to uniform pressure on the inner and outer surface is given by the equation [18] (1951):

$$\sigma_\theta = \frac{c^2 d^2 (P_o - P_i)}{d^2 - c^2} \times \frac{1}{r^2} + \frac{P_i c^2 - P_o d^2}{d^2 - c^2} \quad (18)$$

where

σ_θ = tangential stress at radius r

c = internal radius of the cylinder

d = external radius of the cylinder

P_i = the uniform internal pressure on the cylinder

P_o = the uniform external pressure on the cylinder

The conditions of the present transition test can be considered as follows:

$$\begin{aligned} a &= \frac{1.356}{2} = 0.678 = \text{internal radius (in inches)} \\ b &= \frac{2.920}{2} = 1.460 = \text{external radius (in inches)} \end{aligned} \quad (19)$$

$$P_i = S_L; \quad P_o = 0; \quad r = 1.460 \text{ inches}$$

By substituting these values in equation 18 and solving for S_L :

$$S_L = [(b^2 - a^2)/2a^2]\sigma_\theta = 1.814 \times \sigma_\theta \quad (20)$$

Equations 17a and 20 can be used for finding the lateral stresses in the specimen from the strain gage readings.

The above equations consider the effect of Poisson's ratio of steel in determining the tangential stresses. Anyhow, if the effects are negligible the lateral stresses can be determined from the following equations:

$$\begin{aligned} \sigma_\theta &= e_t \times E_S \\ S_L &= 1.814 \times \sigma_\theta \\ &= 1.814 \times e_t \times E_S \end{aligned} \quad (21)$$

This simplified equation is utilized in calculating the lateral stresses of the specimens in the present study.

But there are certain inherent differences between the actual underground conditions and the conditions obtained in the cell. Consequently some experimental modifications and corrections are required. The most important factor involved is the elimination of the frictional forces developed on the surface of the specimen in contact with the metal surface of the testing cell. In his earlier experiments in the transition test, Serata found that the friction between the cell and the specimen caused a great divergence in the slope of the plastic line of

stress ranging from 21 to 35° instead of the 45° as postulated from the theory. Several experiments were conducted with various friction reducers and finally it was found that a grease-graphite mixture together with two layers of very thin plastic sheet all around the specimen reduces the friction considerably and that the results obtained are satisfactory [14] (1962). The slope of the plastic line of stress obtained under this condition is very near 45°. The same friction reducer is used in the present study.

The rock specimens tested are prepared in the following manner. The specimens are obtained from drill cores which are machined to a diameter of 1.352 inches and to an axial length of 1.33 inches. The ends of the specimen are ground exactly to a flat surface perpendicular to the axis of the cylinder so as to ensure uniform loading. The small imperfections if any existing on the surface of the specimen after machining are filled in with Duco cement and a final polish given. After the specimen has been prepared, a thin film of grease-graphite mixture is applied all over its surface and it is wrapped tightly with two layers of plastic sheets which are also coated with a thin film of grease-graphite mixture on either side. The inner surface of the steel cell and the plungers are also coated with this friction reducer. The specimen in this condition is introduced into the steel cell, taking care to see that the excess of grease is removed and no wrinkles are formed in the plastic sheet. The

plungers are attached on either side of the steel cell and then compressed in the compressing machine. The required electrical connections are given to the strain gages along with the strain indicator.

V. SPECIMEN DESCRIPTION AND TESTING RESULTS

The specimens tested under this new technique of triaxial compression are (1) limestone, (2) sandstone, (3) granite, (4) marble, (5) shale, (6) anhydrite, and (7) rock salt. Specimens (1) to (4) were kindly furnished by Dr. Leonard Obert, U. S. Bureau of Mines, College Park, Maryland. Specimens (5) and (6) were obtained from Michigan State Geological Survey. Specimen (7) was obtained from the salt dome in Louisiana. The specimens are shown in figure 8.

Limestone: The specimen is from Indiana. It is greyish white in color, very fine grained and is composed of small grains of calcite. Five cycles were run on this specimen, up to a maximum loading of 70,000 lbs. The lateral stress - axial stress diagram is shown in figure 9. The plastic line gives an angle of 30° .

Sandstone: This specimen is from Ohio. It is yellowish-brown in color, chiefly composed of fine rounded grains of quartz cemented together in a ferruginous matrix. Five cycles were run on this specimen up to a maximum loading of 95,000 lbs. The lateral stress - axial stress diagram is shown in figure 10. The plastic line shows an angle of 30° .

The specimen was found to be completely crushed when it was ejected from the cell after the experiment.



NOV • 62 •

Figure 8. Photograph of the specimens tested.

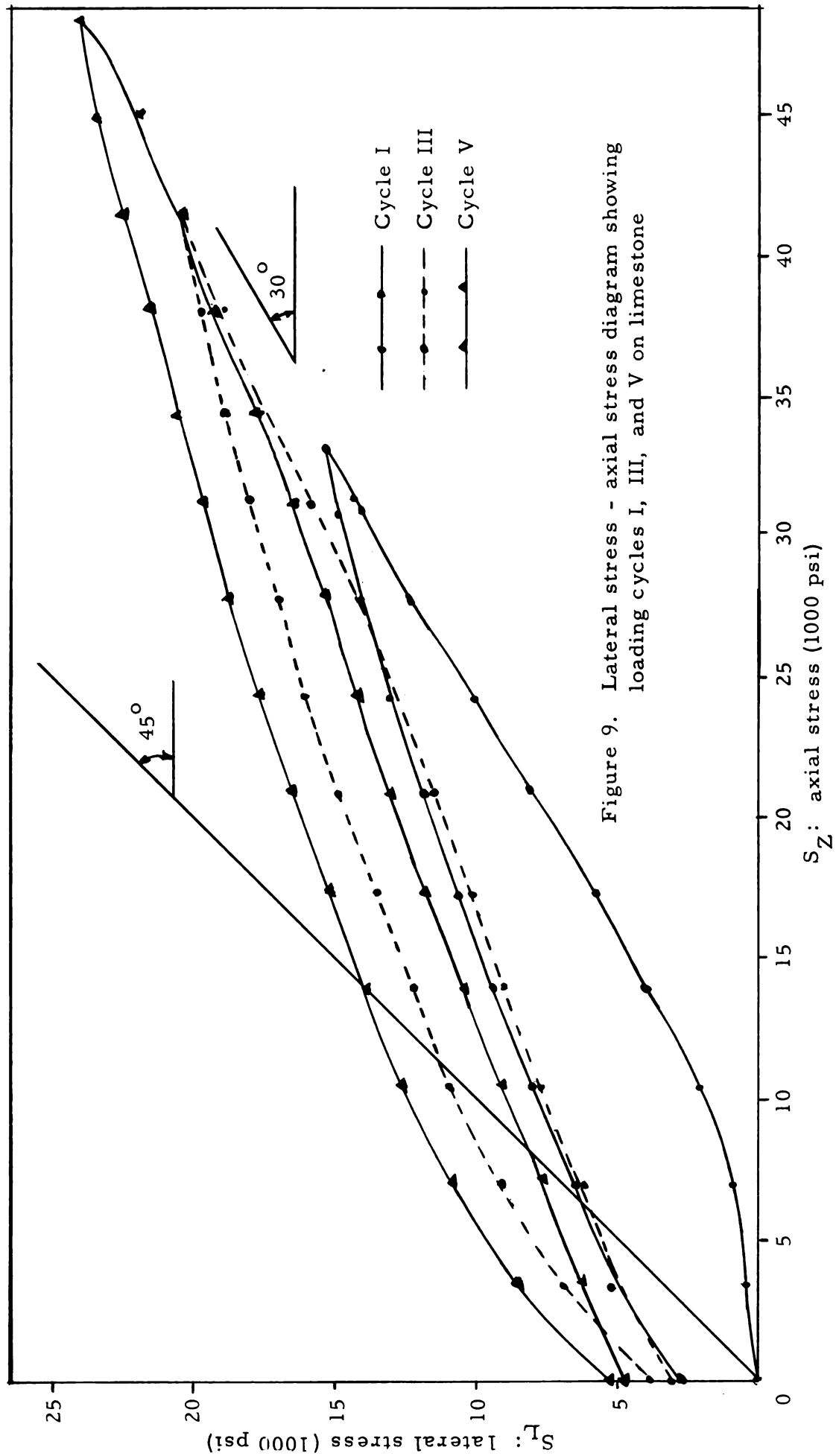


Figure 9. Lateral stress - axial stress diagram showing loading cycles I, III, and V on limestone

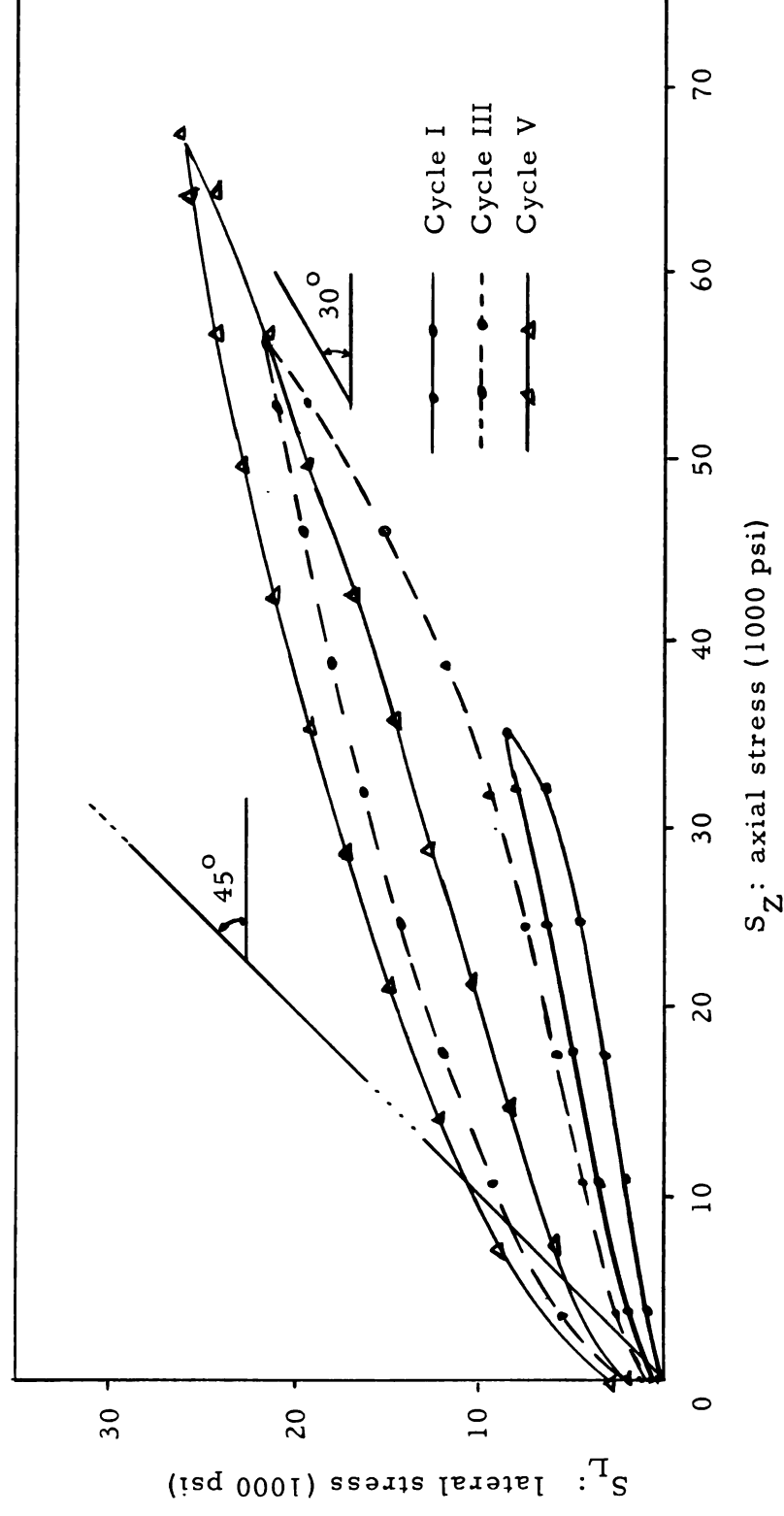


Figure 10. Lateral stress - axial stress diagram showing loading cycles I, III, and V on sandstone

Granite: This specimen is from Deer Island. It is composed of coarse crystal grains of pink orthoclase, anhedral grains of quartz and some small quantities of flaky biotite. Three cycles were run on this specimen up to a maximum loading of 160,000 lbs. The lateral stress - axial stress diagram is shown in figure 11. The plastic line shows an angle of 12° .

The specimen was found to be crushed at the end of the experiment.

Marble: This specimen is from Texas. It is white in color and consists of fine grained interlocking crystals of calcite. Three cycles were run on this specimen to a maximum loading of 160,000 lbs. The lateral stress - axial stress diagram is shown in figure 12. The plastic line gives an angle of 30° .

Poisson's ratio and modulus of elasticity are also calculated for this specimen. These are shown in figures 13 and 14.

Shale: This specimen is from Michigan. It is greyish black in color and is composed of extremely fine-grained argillaceous material. Two cycles were run on this specimen up to a maximum loading of 110,000 lbs. The lateral stress - axial stress diagram is shown in figure 15. The plastic line shows an angle of 25° .

Anhydrite: This specimen is also from Michigan. It is bluish grey in color and extremely fine grained. Three cycles were run on this specimen to a maximum loading of 130,000 lbs. The lateral stress -

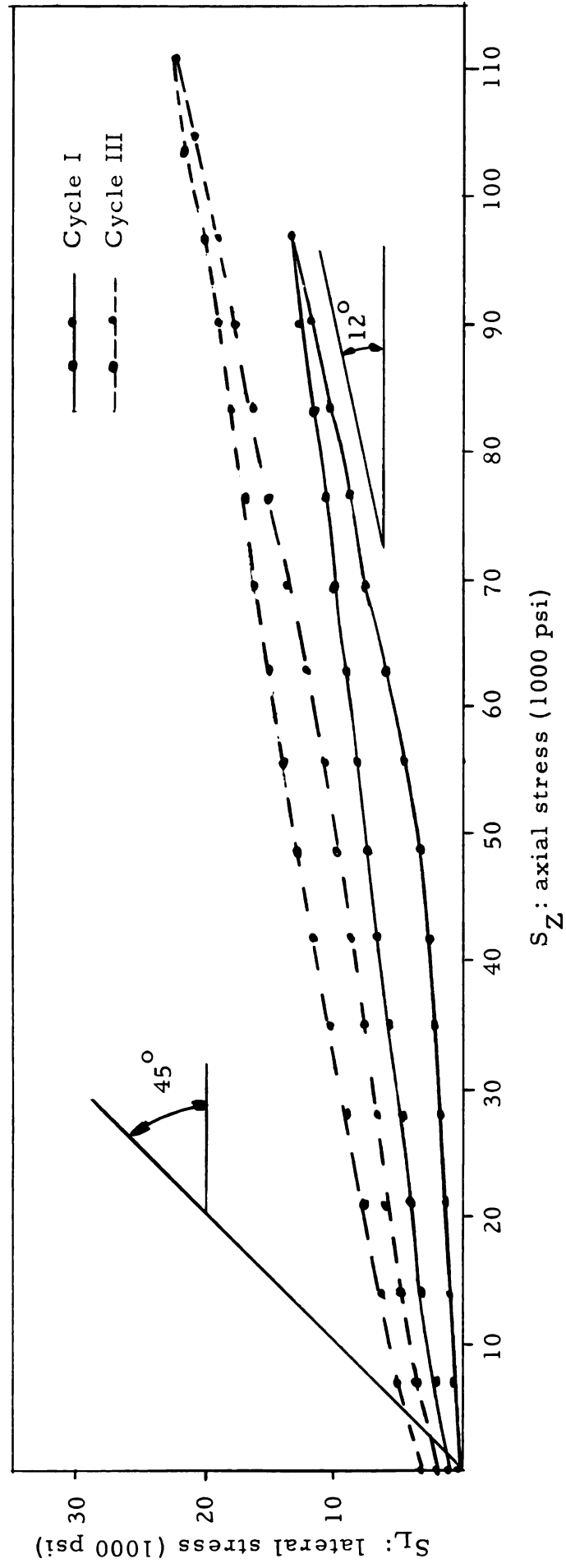


Figure 11. Lateral stress - axial stress diagram showing loading cycles I and III on granite.

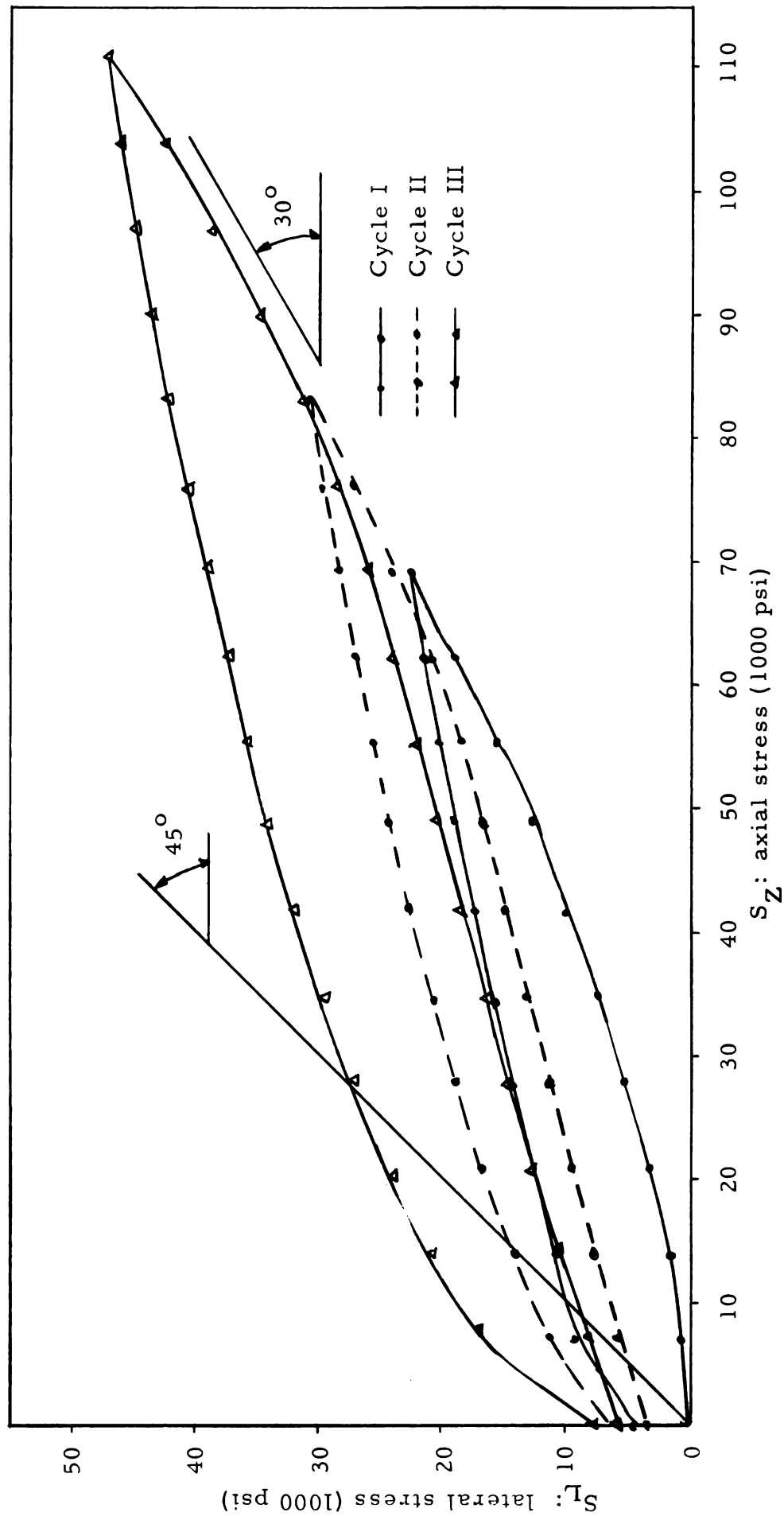


Figure 12. Lateral stress - axial stress diagram showing loading cycles I, II and III on marble

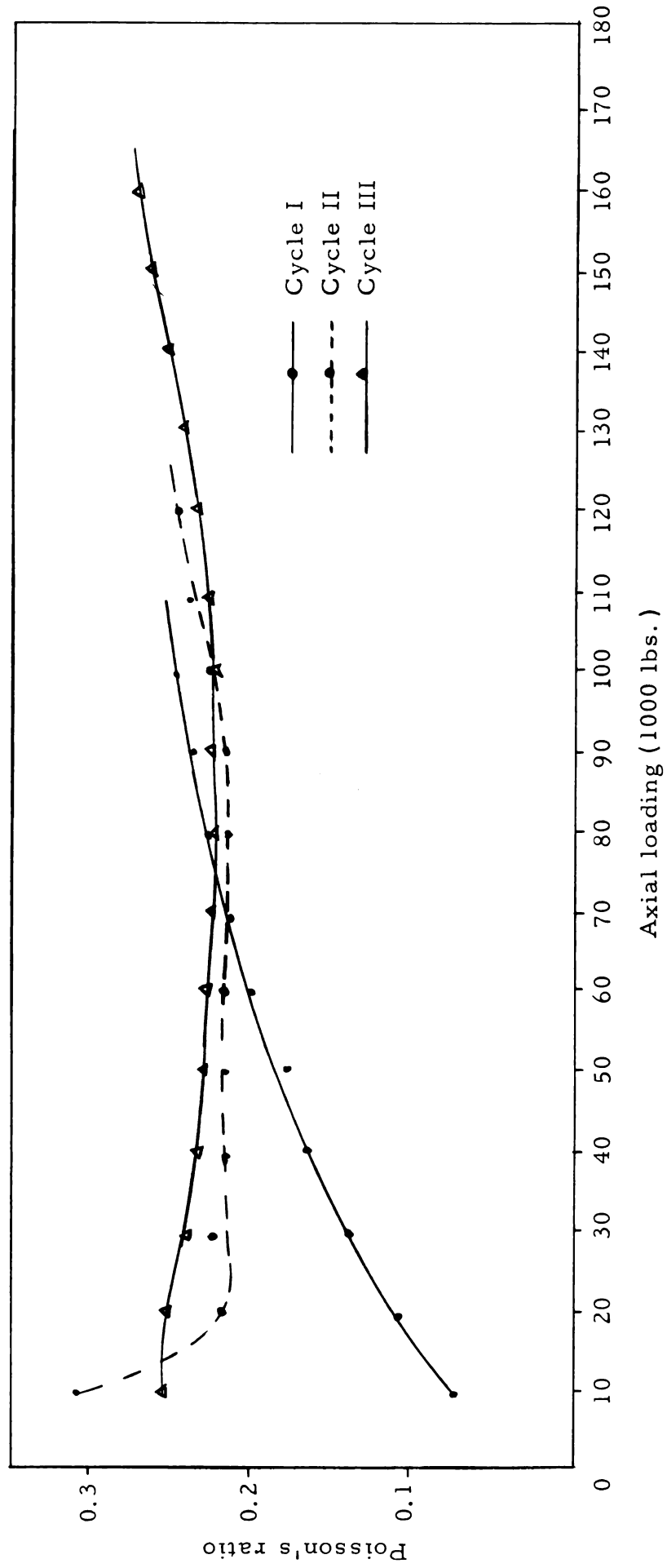
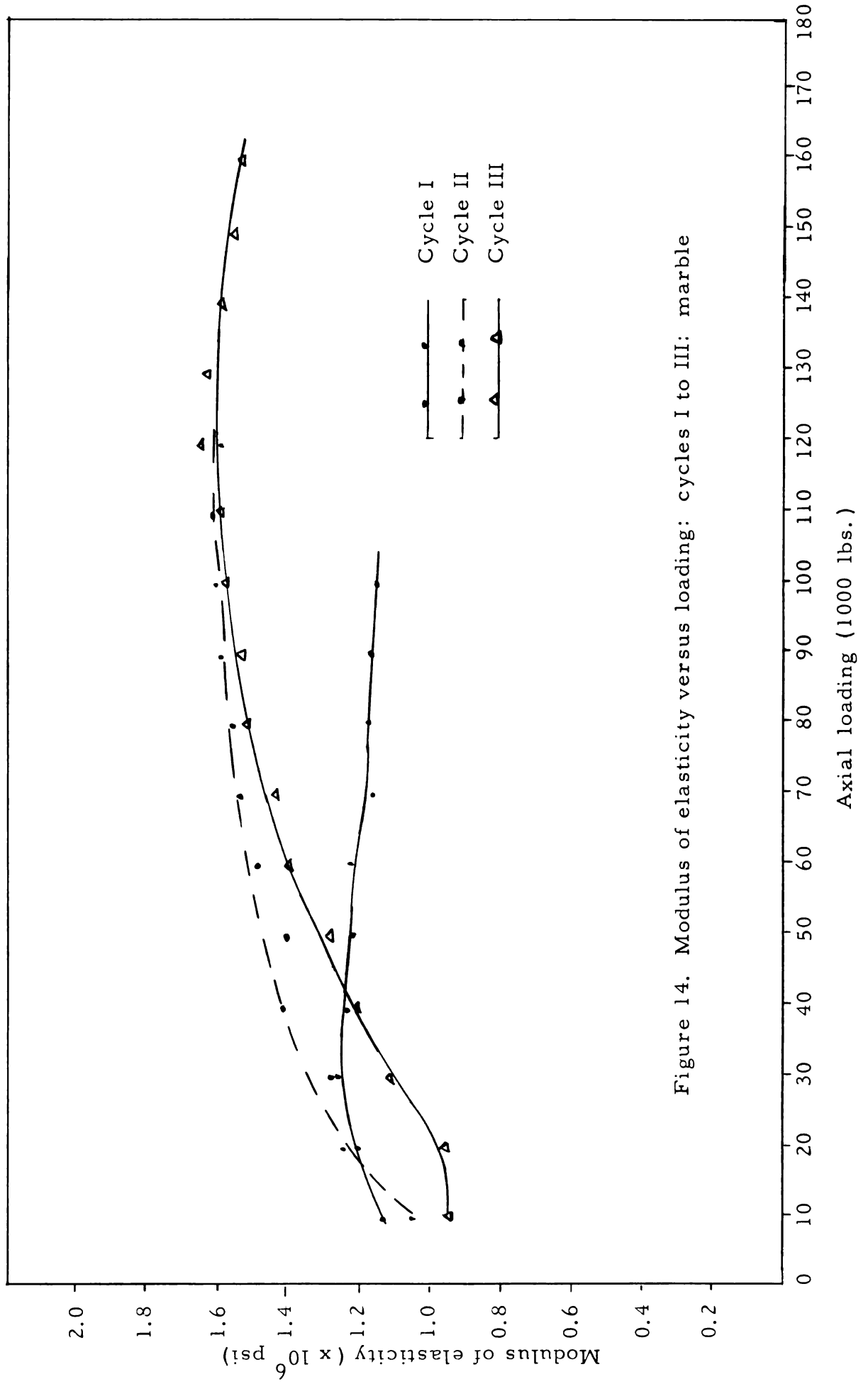


Figure 13. Poisson's ratio versus loading: cycles I to III: marble



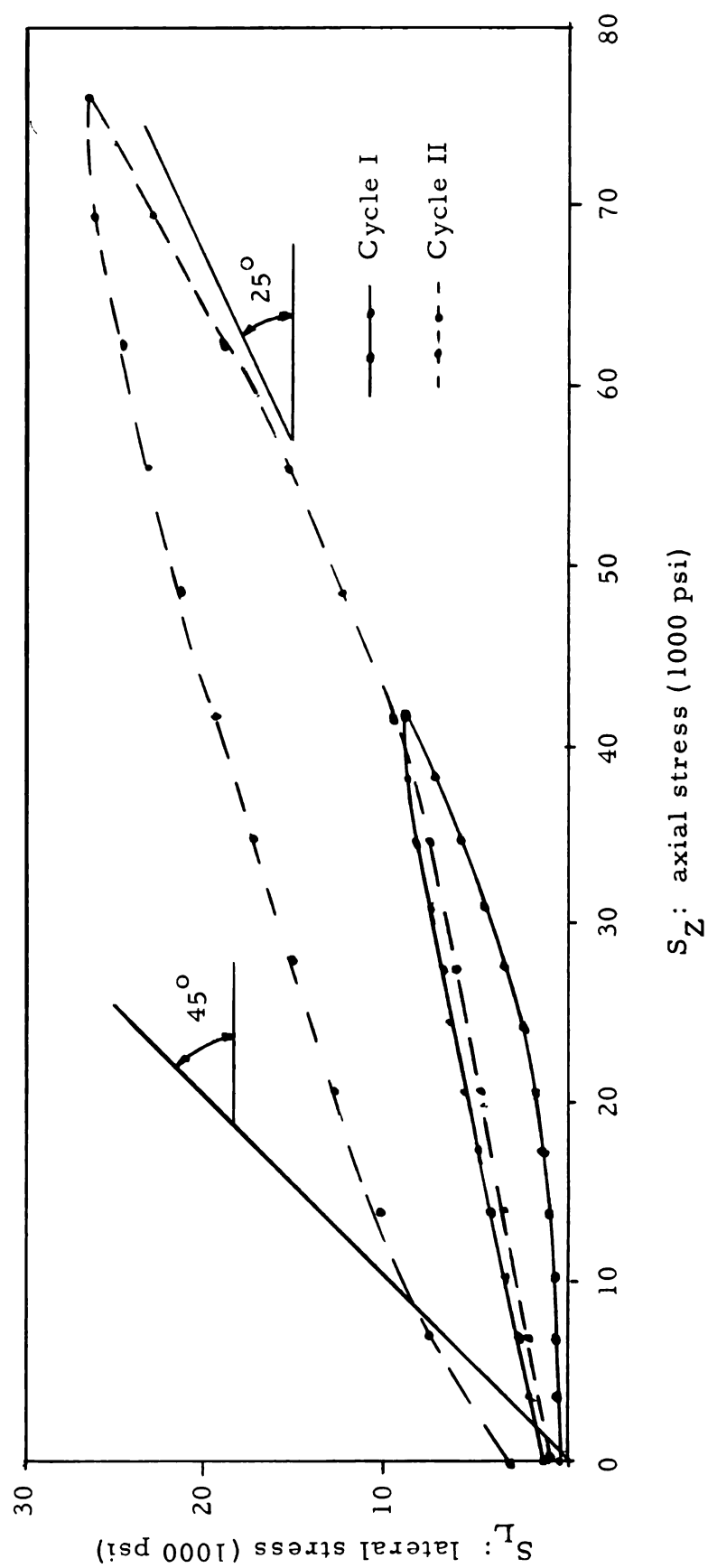


Figure 15. Lateral stress - axial stress diagram showing loading cycles I and II on shale

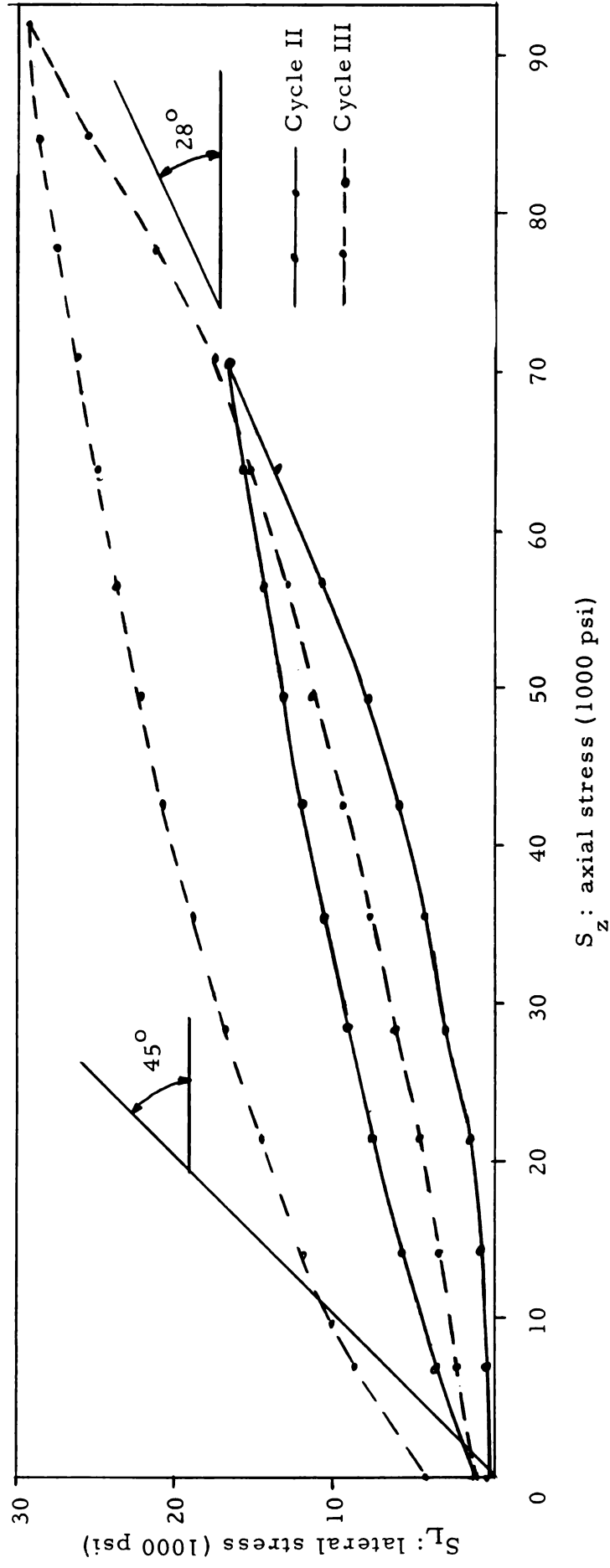


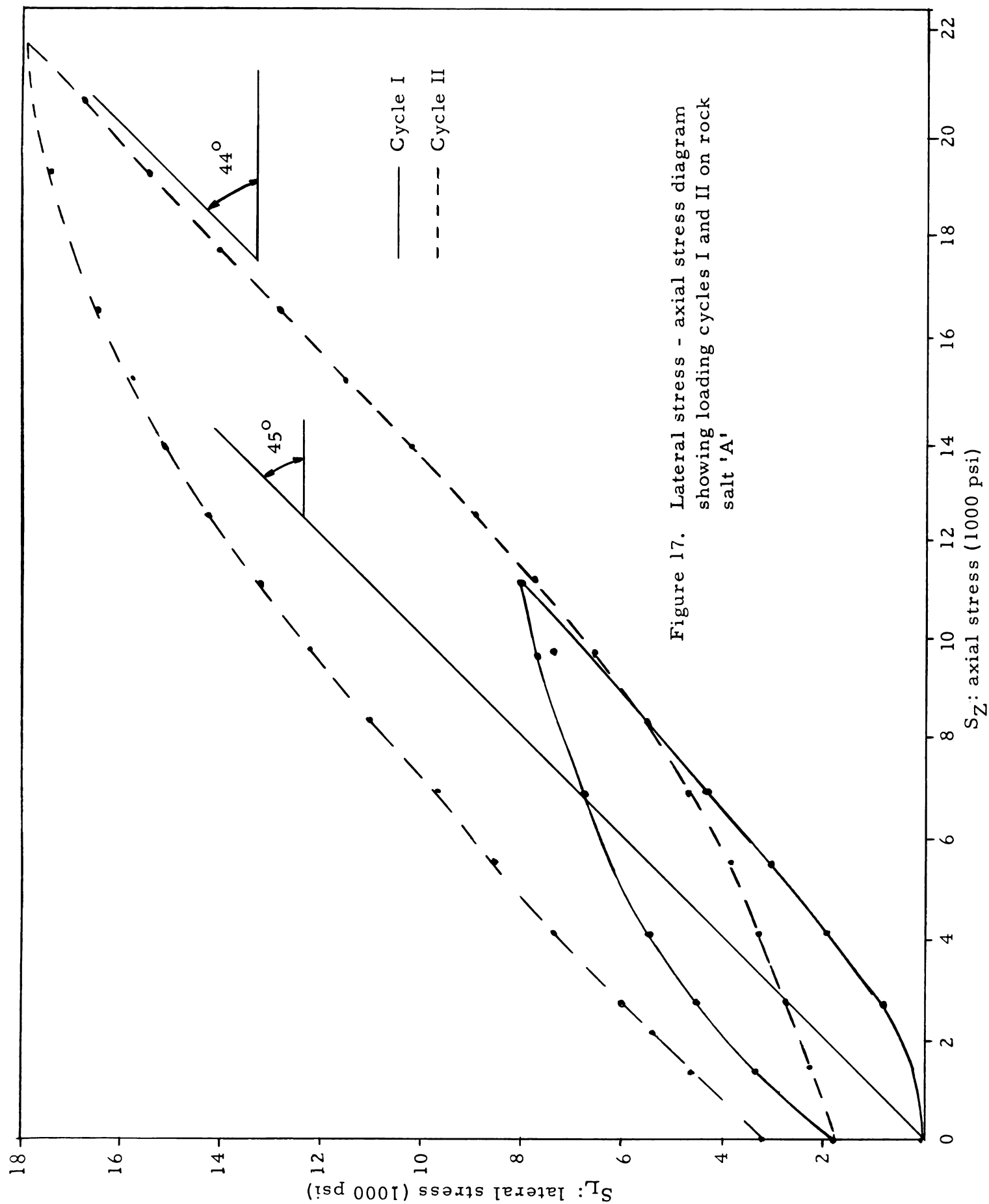
Figure 16. Lateral stress - axial stress diagram showing loading cycles II and III on anhydrite.

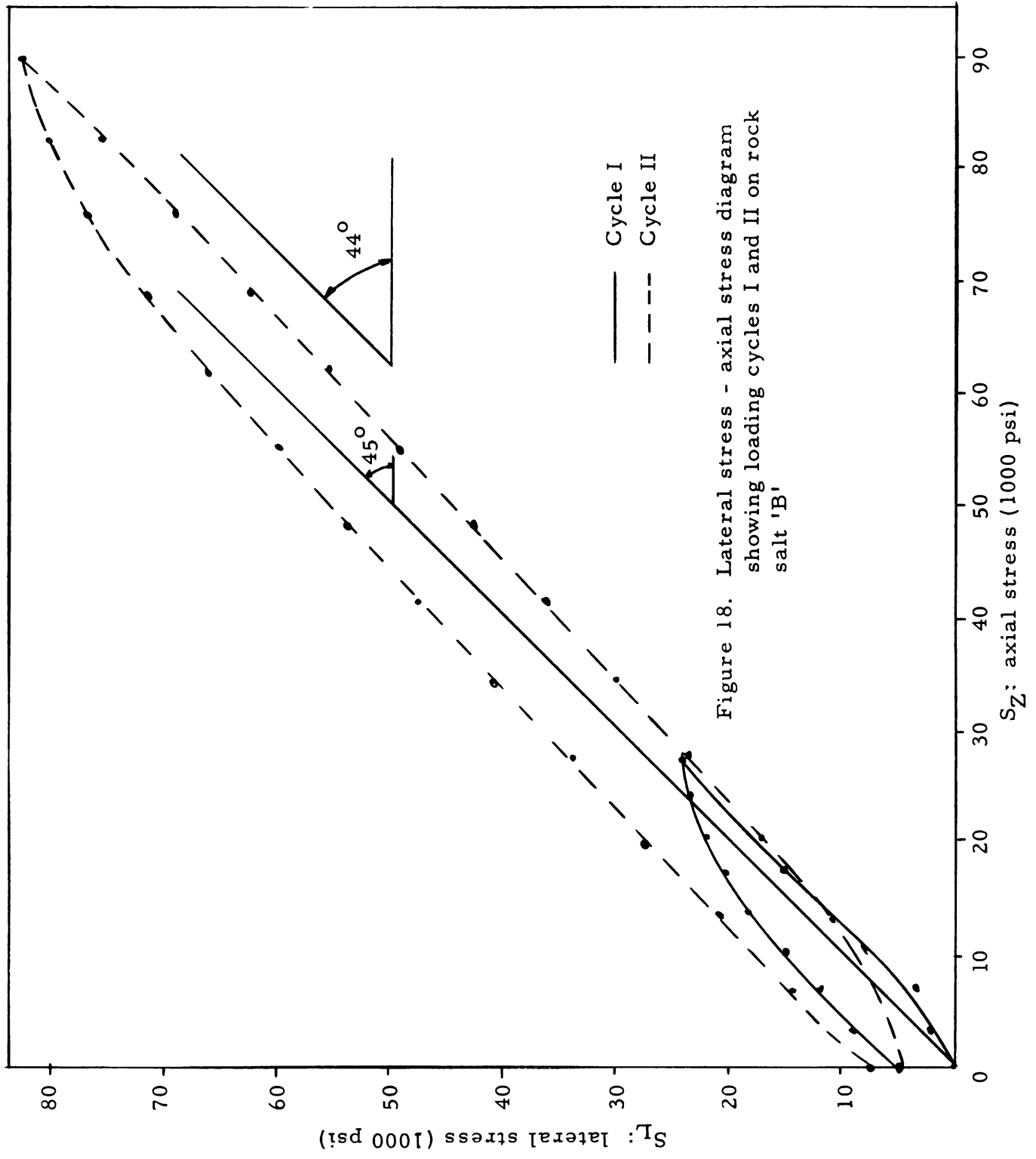
axial stress diagram is shown in figure 16. The plastic line shows an angle of 28° .

On examining the specimen after the completion of the test, it was found to exhibit Luder's lines which are elongated markings that appear on surfaces of some materials when stresses exceed the yield point.

Rock Salt: This is from the salt dome of Louisiana. It is colorless to white in color, composed of interlocking transparent to translucent crystal grains of halite. Two specimens were tested and two cycles were run on each of the specimens up to a maximum loading of 32,000 and 130,000 respectively. The lateral stress - axial stress diagrams are shown in figures 17 and 18 respectively for both the specimens. The angle obtained for the plastic line in both the cases is 44° .

In the lateral stress - axial stress diagrams for the above specimens only selected cycles are represented in some cases in order to avoid congestion in the diagrams.





VI. EVALUATION OF EXPERIMENTAL RESULTS AND DISCUSSION

The theory of experiments as discussed in Chapter III requires that the transition between the elastic and plastic states should be abrupt and the angle β of the plastic line should be 45° .

Even a casual glance at the lateral stress-axial stress diagrams (figures 9 to 12 and 15 to 18) for the various cycles conducted on the different specimens certainly does reveal the trend in transition from elastic to plastic state. The lateral stress - axial stress curves representing the plot for the different cycles of loading can be visualized as a series of parallelograms with pairs of parallel lines corresponding to the elastic and plastic state respectively. The nature of deviation of these curves, though they may not be very sharp, clearly demonstrates the aspect of transition with increasing compression.

The diagrams for rock salt (figures 17 and 18) show more definitely this abrupt transition than any other rock types tested. The rest of them show only a gradual transition. Further, the angle of slope of the plastic line obtained for rock salt is 44° which is in close conformity with the predicted value of 45° . The same result was obtained by Morrison [14] (1962) in his studies on rock salt.

But none of the other rock types examined in this study showed any

angle near 45° for the slope of the plastic line. The angles ranged from 12° in granite, through 25° in shale, 28° in anhydrite, and 30° in limestone, sandstone and marble. Similar deviation was observed by Serata [17] (1961) in his tests on dolomite. He explained the same as due to the effect of incomplete reduction in friction between the testing cell and the specimen. The improved friction reducer, viz., the grease-graphite mixture used by Morrison in his test on rock salt was effective and the same is true in the present study also as far as rock salt is concerned. Morrison's test was restricted to pressures up to 12,500 psi. The effectiveness of this friction reducer may be doubted when the specimens are subjected to very high pressures as in the present study. To test the efficacy of its function at very high pressures, a duplicate sample of rock salt was tested reaching a loading of 130,000 lbs. or about 90,000 psi and it was found to be effective as revealed by the plastic line exhibiting an angle of 44° as shown in figure 18.

The noncompliance of the other rock types to the 45° slope of the plastic line may be due to the nature of the material itself. However, the successive cycles show a slight increase in the angle of inclination and it may be that if extremely high axial stresses are reached, the plastic line may show an angle nearer to 45° . Extremely high pressures were not attempted as they would be beyond the capacity of the testing cell. The maximum loading reached was 160,000 lbs. which amounts to an axial stress of about 110,700 psi on the specimen.

One-third of the normal distance between the plastic lines, if they have a 45° slope, represents the octahedral shearing strength of the material. Excepting for rock salt, as the other rock types in the present study do not show the 45° slope for the plastic line, the distance between them does not represent the true octahedral shearing strength of the material. It may be observed that the distance between them increases in the successive cycles of higher loading. This is thought to be due to the increased strength of the specimen on account of strain hardening.

But the third cycle in granite (figure 11) and the fifth cycle in sandstone (figure 10) do not show the increased distance between the plastic lines. This is due to the specimen having been crushed in an earlier cycle of loading. Still the loop of the stress curves maintains some thickness indicating the internal friction of the powdered media.

The crushing of the granite may be due to a slight space between the testing cell and the specimen. This space might have been greater than the maximum yielding strain of the material. However, in the first cycle on granite, the trend in transition can be noticed. The crushing of the sandstone may also be due to the same cause and further the loose cementing material of the sandstone may also give way under conditions of high pressure.

Further a comparison of the plastic lines indicates that a hard

rock like granite shows a low angle of 12° for its plastic line, while less strong ones show greater angles, and the comparatively weak rock salt shows a high angle of 44° . This can be explained by two factors, viz., the strength of the bonding of the grains and the strength of the individual grains themselves. In the case of granite, though it is found to be crushed in the present study, the strength is still maintained by the individual grains of quartz and feldspar which show only the elastic state under the pressures reached.

Another interesting phenomenon observed in this study is the appearance of Luder's lines on the surface of the anhydrite specimen. These lines appear sometimes on certain minerals when deformed just past their yield point. These markings lie approximately parallel to the direction of maximum shear stress and are the results of localized yielding.

VII. CONCLUSIONS

The work performed in this study strives to apply the transition theory in understanding the behavior of rocks under high pressures, with restraint on lateral expansion. Rocks of varying strength have been examined to evaluate the phenomenon of their change from elastic to plastic state.

Based upon the pressure experiments which were performed the following conclusions may be arrived at.

1. The rock types show a definite trend in transition from elastic to plastic state with increase in pressure, though the change over may not be so abrupt as required by the transition theory.
2. The angle of the plastic line for very strong rocks is low while the weaker rocks show higher angles. Granite shows 12° for its plastic line and the weak salt rock shows 44° .
3. The slope of the plastic line seems to be specific to the individual rocks and it appears to be effected by two factors--bonding of the grains and the strength of the grains themselves. When the specimen is crushed, it forms a new slope. Before crushing the change in slope represents the trend towards the plastic state. After crushing, the nature of the curve is a straight line and there is no change in slope and it means that this slope represents the elastic state for the individual grains.

4. Successive cycles with increased axial stress show an increase in the strength of the specimen which is probably caused by strain hardening.

VIII. SUGGESTIONS FOR ADDITIONAL RESEARCH

Further research on elastic-plastic transition tests on rock types may be carried out on the following lines.

The effect of temperature, time, interstitial solutions and pore pressures may also be studied. Suitable cells must be devised to introduce these variables in the transition test.

The influence of grain size may also be studied by testing rock types ranging in texture from extremely coarse grained to extremely fine grained, as in plutonic, hypabyssal, and volcanic types. Further, the effect of composition from acid to ultrabasic may also be examined.

The contrasting behavior of a single crystal and the same mineral in a fine grained or coarse grained texture in a cemented matrix can also be examined in the transition test. For example, the results of transition test on a single crystal of quartz can be compared with tests on fine grained and coarse grained quartzite. This will enable one to study the effect of bonding between the crystal grains as compared with the strength of crystals themselves in the transition test.

BIBLIOGRAPHY

1. Adams, F. D., and Nicholson, J. T. (1901) "An experimental Investigation into the Flow of Marble," Proceedings of the Royal Society of London, Series A, Vol. 195, pp. 363-401.
2. Adams, F. D. (1910) "An Experimental Investigation into the Action of Differential Pressure on Certain Minerals and Rocks, employing the process suggested by Professor Kick," Journal of Geology, vol. 18, pp. 489-525.
3. _____ (1912) "An Experimental Contribution to the Question of the Depth of the Zone of Flow in the Earth's Crust," Journal of Geology, vol. 20, pp. 97-118.
4. _____, and Bancroft, J. A. (1917) "On the Amount of Internal Friction Developed in Rocks During Deformation and on the Relative Plasticity of Different Types of Rocks," Journal of Geology, vol. 25, pp. 597-637.
5. Balsley, J. R. (1941). "Deformation of Marble Under Tension at High Pressure," Trans. Amer. Geophys. Union, Pt. 2, pp. 519-525.
6. Bridgman, P. W. (1949a). The Physics of High Pressure, London: G. Bell and Sons, 445 pp.
7. _____ (1952). Studies in Large Plastic Flow and Fracture, New York, McGraw-Hill Book Company, 362 pp.
8. Griggs, D. T. (1936) "Deformation of Rocks Under High Confining Pressure," Journal of Geology, vol. 44, pp. 541-577.
9. _____, and Miller, W. B. (1951) "Deformation of Yule Marble I-Compression and Extension Experiments on Dry Yule Marble at 10,000 Atmospheres Confining Pressure, Room Temperature," Bull. Geol. Soc. America, vol. 62, pp. 853-862.
10. _____, Turner, F. J. and Heard, H. C. (1960) "Deformation of Rocks at 500° to 800°C," Geol. Soc. America, Memoir 79, Rock Deformation--A Symposium, pp. 39-104.

11. Handin, J., and Hager, R. V., Jr. (1957) "Experimental Deformation of Sedimentary Rocks Under Confining Pressure: Tests at Room Temperature on Dry Samples," Bull. Amer. Assoc. Petroleum Geologists, vol. 41, No. 1, pp. 1-50.
12. _____, and Griggs, D. T. (1951) "Deformation of Yule Marble. II - Predicted Fabric Changes," Bull. Geol. Soc. America, vol. 62, pp. 863-885.
13. John, K. W. (1962). "An Approach to Rock Mechanics," Proc. Amer. Soc. Civil Engineers, Journal of Soil Mechanics and Foundation Division, vol. 88, No. SM4, Pt. I, pp. 1-30.
14. Morrison, D. M. (1962) "The Transition Test as a Method for Determination of the Mechanical Properties of Materials in a Continuous Medium," Master's Thesis, Michigan State University.
15. Paterson, M. S. (1958a) "Experimental Deformation and Faulting in Wombean Marble," Bull. Geol. Soc. America, vol. 69, pp. 465-476.
16. Robertson, E. C. (1955). "Experimental Study of the Strength of Rocks," Bull. Geol. Soc. America, vol. 66, pp. 1275-1314.
17. Serata, S. (1961) "Transition from Elastic to Plastic States of Rocks under Triaxial Compression," Bulletin of the Mineral Industries Experiment Station, No. 76, Nov. 1961. Proceedings of the Fourth Symposium on Rock Mechanics, College of Mineral Industries, The Pennsylvania State University, University Park, Pennsylvania.
18. Timoshenko, S. and Goodier, J. N. (1951). Theory of Elasticity, New York, McGraw-Hill Book Company, Inc., p. 59.
19. Turner, F. J., and Ch'ih, C. S. (1951) "Deformation of Yule Marble. III - Observed Fabric Changes," Bull. Geol. Soc. America, vol. 62, pp. 887-905.
20. von Karman, T. (1911). "Festigkeitsversuche unter allseitigem Druck," Zeits. Ver. Deut. Ingenieure, vol. 55, pp. 1749-1757.
21. Wuerker, R. G. (1959) "The Shear Strength of Rocks," Mining Engineering, Vol. 11, no. 10, pp. 1022-1026.

ROOM USE ONLY.

ROOM USE ONLY.

AB. 0. 1. 87.

MICHIGAN STATE UNIVERSITY LIBRARIES



3 1293 03175 7580